Reversible and dynamical control of aggregation and soft adhesion of T-responsive polymer-coated colloids

Giuseppe Boniello, Jérémy Malinge, Christophe Tribet, Emmanuelle Marie, Dražen Zanchi

Reversible and dynamical control of aggregation and soft adhesion of T-responsive polymer-coated colloids

Giuseppe Boniello[a], Jérémy Malinge[a], Christophe Tribet[a], Emmanuelle Marie[a], Dražen Zanchi[a,b,*]

[a] *Ecole Normale Supérieure-PSL Research University, Dpt Chimie, Sorbonne Universités - UPMC Univ. Paris 06, CNRS UMR 8640, 24 rue Lhomond, 75005 Paris, France*
[b] *Université de Paris VII Denis Diderot, 5 Rue Thomas Mann, 75013 Paris, France*

Abstract

Colloids with aggregation and adhesion properties reversibly tunable by shift of pH, T, light etc. can be designed by deposition of stimuli-responsive polymer chains on the particle surface. The aim of this work was to investigate how to control the strength of temperature-triggered attraction by analysing self-aggregation kinetics and soft adhesion of colloids to a flat substrate. In order to endow the colloids with reversible and temperature-controlled interactions, silica or polystyrene microbeads (d =200 nm and 1 μm) were coated by mixed solutions of poly(lysine)-grafted-polyethylenoxide (PLL-g-PEG, for steric repulsion) and PLL-g-PNIPAM (i.e. PLL with poly-N-isopropylacrylamide T-responsive side chains). PEG-coated particles were stable in suspension, while the presence of PNIPAM provoked, at $T > T_c = 32 \pm 1°$C, reversible aggregation and/or adsorption on glass plates. Dynamic light scattering following a T-jump from 25°C to 40°C was used to measure the aggregation rate and corresponding stability ratio W. For a molar fraction of PLL-g-PNIPAM, f, ranging from 100% down to about 20%, particles aggregate rapidly with slowly increasing W. Below $f \approx 20\%$, W increases by 3 orders of magnitude. The real-time 2D tracking method was used to monitor (x, y) positions of particles in suspension above microscope glass slides during a T-triggered adsorption. In

*Corresponding author
Email address: zanchi@ens.fr (Dražen Zanchi)

order to capture transitory dynamics near PNIPAM collapse transition, particles tracks were recorded within a T-ramp of 10°C/min from below to above T_c. The particle-substrate interaction was found to hinder the near-wall diffusion and provoke the soft adhesion, as revealed by observation of characteristic confined Brownian motion. Resulting confinement potential stiffness profile $\alpha(f)$ presents a crossover from constant to linearly increasing at $f \approx 20\%$. Altogether, the characteristic coverage $f^* \approx 20\%$ is interpreted as a crossover from discrete to continuous coverage pattern within the soft contact domain.

Keywords: Colloids, temperature responsive polymers, PNIPAM, soft adhesion, Brownian motion, aggregation

1. Introduction

Self-association and soft adsorption dynamics of polymer-coated colloids attract considerable attention in studies of bottom-up designed composite materials [1], colloidal crystals [2], bacterial adhesion [3], biofouling resistant devices [4] etc... Controlled interactions with the solid phase can be also involved in a field-flow separation approach [5, 6]. Reversible and dynamically tunable, or even time-modulated, interactions are prerequisite for other, far-from-equilibrium colloidal assemblies [7, 8]. External stimuli typically used for tuning surface, dynamical and/or interactions in colloids are light [9], electric [10] and magnetic [11] fields, pH [12, 13, 14], solvent [15, 16] or temperature variation [17]. Tunable aggregation and/or adhesion, triggered by external stimuli, may entail benefits for the uprising class of functional materials. In this respect, stimuli-responsive colloidal particles find applications in controlled stabilization, destabilization and inversion of emulsions, foams and suspensions [18], in tunable catalysis [19, 20], and in temperature-sensitive colloidosomes [21].

In the present paper we report results on self-aggregation and soft adsorption on flat surface of colloids endowed with T-responsive polymer coating with controlled interaction strength. The temperature of the sample is easily controlled and tuned by using thermostated cells (for particle-particle study) or

Peltier elements and heating stages. On the other side stimuli-responsive polymer coating can be used as an efficient mean to control their surface properties and induce stimuli-sensitive behaviour [22]. Since we are interested in temperature-dependent mechanisms Poly(N-isopropylacrylamide) (PNIPAM) is used. PNIPAM-coated particles undergo temperature-triggered collapse transition above a critical temperature $T_c \sim 32°$C [22, 23, 24, 25]. A robust experimental strategy enabling a facile preparation of coated particles has been proposed in a recent work [26]. The method consists in the use of cationic comb-like poly(Lysine) derivative as a versatile platform to deposit functional strands on anionic particles. The PLL-graft-PEO has been extensively studied (and is now commercialized) for its excellent bio-repellency that is effective on a broad variety of surfaces (metals covered by a thin oxide layer, plasma-cleaned polymers including PS and PDMS, glass, ceramic, etc). We here broaden the family of this interesting polymer, by addition of T-responsiveness. It is likely that other polymers (diblock) may achieve similar properties, but it is not always the case: for instance, alternative architectures (such as grafted poly(ethyleneimine)) make poor adlayers, prone to locally attractive (cationic) micro-defects. The polycationic PLL backbone ensures tight Coulomb attachment onto anionic surfaces (glass, plastics, silicium) [4, 27, 28, 29]. Different side chains can be grafted on such PLL backbones. For the purposes of the present work we used poly-N-isopropylacrylamide (PNIPAM) and polyethylenoxide (PEG). PLL-g-PNIPAM, provides the thermo-responsive behaviour required for reversibly switched colloidal interactions. PLL-g-PEG endows surfaces with steric repulsive shield in the whole range of working temperatures. At $T > T_c \sim 32°$C PNIPAM chains collapse to give way to particle-particle and particle-substrate attraction. The strength of this interaction is itself tunable by adjusting PLL-g-PNIPAM molar ratio f in the coating. Thus, our system is determined by two control parameters T and f.

The aim of the present analysis is to explore the possibilities to control the strength of the T-triggered interactions between polymer-coated colloids. We used dynamic light scattering to monitor the aggregation kinetics following a

T-jump from 25°C to 40°C. Aggregation rate in the very beginning of kinetics allowed us to extract the stability ratio W. The adsorption of particles on a flat surface in a slow T-ramp was studied by 2D particle-tracking using a microscope and a camera. The resulting tracks were analysed to yield the mean square displacement (MSD), which, in turn, was fitted to the Langevin equation of a Brownian particle in harmonic confining potential. In Section 2 we describe materials and methods. Section 3 reports on the particle-particle interactions, i.e. the colloid destabilisation – re-dispersion cycles in a series of ascending – descending T-ramps and the DLS results in T-jump experiments. Section 4 focuses on the particle-surface interactions leading to the adsorption process and subsequent Brownian dynamics of softly adhered beads. Section 5 contains discussion of the f dependence of aggregation stability ratio W and soft adhesion stiffness α. Conclusions and implications of our results are given in Section 6.

2. Materials and methods

Particles self-association. Commercial carboxylated polystyrene microspheres (Polybead, Polyscience, 200 nm in diameter) were dialysed against water (Slide-A-Lyzer, M_W cutoff 3500 kDa, Thermo Scientific). The solution was diluted in 5 mM phosphate buffer. Particle coating was obtained mixing $13\mu L$ of beads in PBS with $60\mu L$ of polymer solution $10g.L^{-1}$ (f% PLL-g-PNIPAM, $(100-f)$% PLL-g-PEG) in 5 mM phosphate buffer. (PLL: $M_w = 15000 - 30000g.mol^{-1}$, grafting density 20%; PEG: $M_w = 2000g.mol^{-1}$, $R_g = 1.8$ nm; PNIPAM: $M_w = 2000g.mol^{-1}$, $R_g = 1.8$ nm). Polymer chains adsorb on the particle surface up to saturation density (typically of the order of 1.1 mg m^{-2} [29, 4], not measured for present system). The resulting suspension was incubated for 5 min. Polymer excess was removed by size exclusion chromatography (Sephacryl HR 300 column, 2.5 x 1.5 cm) pre-equilibrated with 5 mM phosphate buffer. Typical retention volume of polymer-coated beads was 1.1 mL, making the beads well separated from excess unbound polymer (retention volume of 2.4 mL). The efficiency of the protocol to obtain a controlled f has been ensured by fluores-

cent measurements on rhodamine-modified-PLL-g-PNIPAM [26]. Accordingly, the PEG-to-PNIPAM ratio in coating remains indeed the same as the one in the co-polymer solution before adsorption. The 1 mL samples prepared at room temperature ($T = 25°$C) were plunged in the thermostated cell ($T = 40°$C) of DLS apparatus (Brookhaven BI-200SM equipped with a multiple tau digital correlator and a 30 mW diode laser operating at 637 nm). The scattered light intensity was measured at 90° scattering angle. Temperature control within 0.1°C was achieved using a bath circulator connected to a temperature probe plunged in the decalin bath nearby the sample cell. The temperature of the sample attains 32°C within seconds and the aggregation takes place. The effective hydrodynamic diameter (second cumulant) was monitored in time. ζ-potential were measured in a Zetasizer (Nano ZS, Malvern Instruments Ltd) equipped with a He-Ne laser and temperature controller (±0.1°C). Five measurements were recorded and their standard deviation is reported.

Particles adsorption on a flat substrate. Silica beads ($0.96\mu m$ in diameter, Bangs Laboratories, SS03N) were dispersed in sodium hydroxide solution 1M by sonication for 15 min and dialysed against water (Slide-A-Lyzer, M_W cutoff 3500 kDa, Thermo Scientific). The solution was diluted in 10 mM phosphate buffer. Particle coating was obtained mixing $22\mu L$ of beads in PBS ($18g.L^{-1}$) with $100\mu L$ of co-polymer solution $10g.L^{-1}$ (f% PLL-g-PNIPAM, $(100-f)$% PLL-g-PEG) in 10 mM phosphate buffer. (PLL: $M_w = 15000 - 30000g.mol^{-1}$, grafting density 20%; PEG: $M_w = 20000g.mol^{-1}$, $R_g = 6.9$ nm; PNIPAM: $M_w = 7000g.mol^{-1}$, $R_g = 3.8$ nm). Polymer chains adsorb on the particle surface up to saturation density. The resulting suspension was incubated for 30 min. Polymer excess was removed by 5 centrifugation cycles (1.800g for 5 min) replacing the supernatant with deionised water.

The flat substrate consisted in a borosilicate glass microscope slide (thickness=0.17 mm) cleaned with ethanol and sonicated for 30 min in a 1M sodium hydroxide. After rinsing with deionised water, the experimental cell was prepared by superposing bi-adhesive tape and a mylar film. A 52 mm x 5 mm x 50μm channel was thus created between the borosilicate glass slide and the

mylar film. The bottom of the channel was coated with PLL-g-PEG ($M_w = 20000 g.mol^{-1}$) by injecting co-polymer solution ($1 g.L^{-1}$ in 10 mM phosphate buffer) in the cell and left to incubate for 30 min. The cell was then rinsed with deionised water and dried by compressed air. Note that the flat substrate thereby prepared was not thermo-sensitive and had no active role in particle adhesion. In fact, the full PLL-g-PEG coating ensured a steric repulsion with particles of whatever the coating when the T-stimulus is absent. The T-ramp experiments were performed using a temperature controlled microscope stage (Linkam PE94). The particles suspension were injected into the cell at $T = 26°$C and subjected to a temperature ramp of 10°C/min up $T = 36°$C. The beads are observed by Phase Contrast Microscopy (Leica DM IRE 2) equipped with objective (Leica HCX Fluotar L 63x/0.70) and a CMOS camera (iDS uEye CP, pixel size=0.12μm). Particles were tracked in real time by Pico-eye software [30] allowing sub-pixel resolution ($\sim$ 5 nm) at 50 frames/s and the mean-square displacement (MSD) was extracted from particles track record using a home-made numerical routine. The MSD profiles were averaged over typically 5 different particles tracks.

3. Particle-particle interaction

Reversibility. Temperature-triggered aggregation, with emphasis on reversibility issue, was studied for f =100% PLL-g-PNIPAM (complete particle surface is thermo-sensitive) by UV-vis spectroscopy, dynamic light scattering (DLS), and zetametry. An indicator of the aggregation is the abrupt decrease of transmittance at 650 nm at $T \simeq 32°$C (blue line in Fig.1a). DLS provides the same information from a quantitative point of view: the suspension is stable below 32°C (the initial diameter is kept constant at 200 nm), larger aggregates show-up above the transition temperature (red line in Fig.1a). Bare particles as well as these without PNIPAM ($f = 0$) [26] were all stable in suspension at all experimentally accessible temperatures. Zetametry experiments, Fig.1b), confirmed the temperature-dependent surface properties. At $T < 32°$C, the weakly

negative potential (- 5 mV) reflects the strong shielding provided by tethered PNIPAM chains. Above PNIPAM collapse transition, the shielding becomes ineffective. On one side the shear plane is moved closer to the surface of the beads, which affect ζ-potential. On the other side, the collapsed PLL-g-PNIPAMs cannot compensate the negative charge from carboxylate ions of bare PS particle surface [29, 4]. The two combined effect results in the decrease of ζ-potential at $T > 32°$C (Fig.1b). However, these potentials are not able to stabilize or destabilize the suspension showing that the leading role in particle-particle interaction is played by the increasing hydrophobicity of PLL-g-PNIPAM with the temperature. Several heating/cooling cycles in the range 23°C-38°C reveal the reversible behaviour of particle-particle aggregation (heating) and re-dispersion (cooling) (Fig.1c).

The role of PLL-g-PNIPAM surface coverage fraction f. The beads were coated with PLL-g-PNIPAM/PLL-g-PEG mixtures as described in Materials section. Each particle batch was characterised by its PLL-g-PNIPAM surface coverage f. The aggregation kinetics were monitored via DLS measurements for a range of coverages f. The evolution of the hydrodynamic diameters as a function of elapsed time spent at $T > T_c$ indicates that the temperature-induced aggregation is in progress. At fixed bead concentration ($10\mu gL^{-1}$) different slopes, i.e. different growth rate of hydrodynamic diameter, suggest that the probability of sticky collision between coated beads increased with the amount of PLL-g-PNIPAM patches (Fig.2).

The colloid aggregation is described by an effective Smoluchowski theory [31] with the f-dependent stability ratio W, defined as the number of overall particle-particle random collisions divided by the number of collisions leading to aggregation. Accordingly, the stability ratio W (Fig.3) determines the initial, linear aggregation kinetics, Fig.2 by:

$$D_h(t) = D_0 \left(1 + \frac{\alpha t}{\tau W}\right)$$

where $D_h(t)$ is the mean hydrodynamic diameter at time t, $D_0 = 200$nm

is the initial particle diameter, α is a numerical pre-factor of the order of 1, and $\tau = \frac{3\eta}{4k_BTc_0}$ is the universal diffusion limited aggregation time (η stands for viscosity, k_BT for thermal energy and c_0 for the number of particles per unit volume). The profile $W(f)$ reveals two regimes of aggregation kinetics: (i) for $f < f^* \sim 20\%$ the patches act as discrete objects while (ii) for $f > f^* \sim 20\%$ the surface of colloids can be seen as mixed brush. For these purposes it is useful to introduce, the concept of contact radius r_c between particles [3], defined by the maximal portion of the sphere that can interact with the surface, either by steric or electrostatic means. When $r_c < a$ (typical distance between PLL-g-PNIPAM patches), W is affected by rotational search of patch-substrate contact, while for $r_c > a$, since whatever the contact point the interaction surface contains some patches, W can be seen as effective translation-diffusion driven one renormalized by relatively rapid searching time among patches within the interaction surfaces.

4. Particle-substrate interaction and dynamics of softly confined particles

In this section we report the results obtained using a simple method to trigger in a controlled way the attractive interactions between the colloids and the flat substrate, which made possible the observation of Brownian dynamics before and after adsorption, including the very event of particle stopping. For this purpose we used real-time tracking within a temperature ramp. The advantage of temperature ramp experiments is that we are always sure to catch the conformational transition in PNIPAM, i.e. the repulsive-attractive switch on particle surface, even without a fine control on the cell temperature. Another advantage is that the moment of PNIPAM conformational transition can be estimated if many particles are in observation window: we are sure that this transition occurs just before the first particle is adsorbed. At the beginning of acquisition the temperature of the stage is 26°C and the T-ramp 10°C/min. allows for a comfortable acquisition, still being slow enough not to interfere with PNIPAM transition kinetics itself. In the beginning of T-ramp all particles undergo a free

2D Brownian motion because of repulsive steric particle-surface interactions. At the end of acquisition the same particles are attached on the substrate, and free diffusion is not observed anymore. This behaviour is reversible, as observed in a decreasing ramp in the same temperature range (data not shown).

Once adsorbed on the surface, the particles have observable confined fluctuations, as seen in the inset of Fig.4. Fluctuations for particles adsorbed at the substrate at a constant temperature $T = 36°\mathrm{C}$ are recorded in real time by *Picoeye* software [30] (sub-pixel resolution ~ 5 nm, acquisition rate 50 frames/s) and statistically analyzed. The distributions of particle position (Fig.5a) depend on the amount of PLL-g-PNIPAM on the particle surface. It is important to notice that the overall experimental noise (other than particle motion) in the (x, y) track contributes by an amount certainly lower than (or equal to) the narrowest observed distribution ($f = 100\%$). Consequently we are sure that any wider distribution are dominated by the stochastic dynamics of the bead softly attached to substrate. MSDs as a function of time lag τ for a range of PNIPAM coating fraction f (Fig.5b) give a complete picture of particle fluctuations. At small timescales, MSDs are linear functions of τ, signature of motion induced by thermal excitation. At longer times, MSDs at all particle coatings reach a plateau, given by confinement potential, which is due to soft adhesion of PEG free chain ends to the regions where PNIPAM went hydrophobic. The profile $MSD(\tau)$ and the confinement range (plateau position) strongly depend on f: the strength of the anchoring is related to the number of PLL-g-PNIPAM blocks that are involved. For a more quantitative analysis, we fit the MSD profiles with the solution of Langevin equation in presence of a parabolic potential well $U(x) = \frac{1}{2}\alpha(x^2 + y^2)$:

$$MSD(\tau) = \frac{k_B T}{\alpha}\left[1 - \exp\left(-\frac{2\alpha}{\gamma}\tau\right)\right] , \tag{1}$$

where $\gamma = 6\pi\eta R$ is the viscous friction, η being the water viscosity. In Figure 5b) the calculated best fitting curves are plotted together with $MSD(\tau)$ profiles extracted from the (x, y) tracking. The corresponding values of the stiffness $\alpha(f)$ are shown in Fig.6.

5. Discussion

The temperature response of core-shell particles covered by PNIPAM, and reversibility (namely hysteresis) after excursion at high T, has been regularly an issue in the control of solubility of particles. A recent report by Scherman [32] indicates that pure PNIPAM-AuNPs (i.e., no free PNIPAM in solution) do not aggregate, presumably because of intra-corona collapse at high surface coverage with PNIPAM. We point out that we purified our particles by similar means as Scherman, to remove free unbound polymers from the solutions. On the other hand, PNIPAM precipitation is typically reversible, but usually prone to large hysteresis (dissolution occurs at T lower by several °C than aggregation). This is not the case of our system, which suggest that inter-particle tight bridging is not as effective as with conventional long PNIPAM chains [33].

The presence of PNIPAM on the surface of a colloid is able to induce attraction at high temperature ($T \gtrsim T_c$), which provokes the self-aggregation and substrate adhesion. In both cases, the molar ratio of PLL-g-PNIPAM which covers the surface (expressed by the parameter f) tunes the strength of the interaction. For particle aggregation this means that the effectiveness of sticky collisions, and consequently the kinetics of aggregation, is affected by f. In the case of particle adsorption f changes the stiffness of the elastic trap where the bead is confined. Here we will discuss the most important two results in this regard. The first result is that the self-association stability parameter as function of f has two well distinguished regimes, delimited by the crossover at $f = f^* \simeq 20\%$, see Fig. 3. The second result is that the harmonic confinement potential stiffness α present a crossover at similar value of f^*, see Fig. 6. In both geometries two regimes are characterised as i) $f \lesssim f^* \simeq 20 - 25\%$ where the properties slightly depend on f; ii) $f \gtrsim f^* \simeq 20 - 25\%$, where the reference parameter (W for aggregation, α for adhesion) is linear in f. A tentative explanation comes from the possible arrangement on PLL-g-PNIPAM blocks on the bead. At low polymer concentration it is very likely that PLL-g-PNIPAM blocks would be isolated (Fig.7a). A finite number of them would be involved in the

aggregation/adsortion process. At high concentration a continuous distribution is obtained (Fig.7b). The effect is proportional to the number of polymer blocks involved in the contact region. By using percolation argument an approximated threshold between the two regimes can be found around $f \simeq 25\%$ (Fig.7c), in agreement with experimental observations in both addressed systems.

Let's put our findings in the context of actual research on soft adhesion inspired by biological phenomena of the cell-surface adhesion or the receptor-drug docking. The dynamics of surface adhesion of micro-particles in a shear flow has been recently studied by [34]. Interesting transient regime was found, between fast drift regime, in which particle is carried by the stream without any contact with the wall, and the arrest of the particle against the wall. In this intermediate regime the particle movement can be interpreted as rolling (or crawling) over the surface. The contact adhesion allowing for a rolling-and-no-slipping constraint, is made possible by continuous attachment detachment of polymer-surface weak links. Interestingly, the theoretically studies of slipping and rolling of cells [35] and of soft adhesion by elasto-hydrodynamical effects [36] interpret the transient states as highly non-trivial phenomena in which the tether-ligand searching time, the rigidity of tethers, together with the lubrication effect in the narrow space between bead and the substrate determine collectively the ageing dynamics in the very last moments before the soft attachment. The relevance of diffusion limited sticking events between polymer head and the substrate has been pointed out already in the context of binding between two surface-tethered reactants in relative motion[37].

Cited works, focused mainly on the shear-driven adhesion, allow us to define some perspectives of the T-ramp approach. These works point out to the rolling (or crawling) phase of the adhesion in the shear flow. During this phase the particle-substrate contact domain explores a considerable fraction of the particle surface. If the flow is added during the sticky phase of our system, particles with stronger adhesion will roll less and vice-versa. The separation procedure could be further optimised by subjecting the system to a series of ascending and descending temperature jumps.

Our experiment in T-ramp can be also compared to the experiments by Kumar *et al.*[38], in which the particle was initially held by an optical trap above a weakly sticky surface, released, and the subsequent motion was then followed by different means. In our approach, the initial position of the particles is the one that particle have in the moment $t = t_0$ when $T = T_c$. Consequently, the initial positions are distributed over some equilibrium profile $\sim e^{-V(z)/k_B T}$ in repulsive surface-particle potential $V(z)$. Immediately after the transition $V(z)$ turns attractive and all particles find themselves in a transitory state, following all adhesion steps. In this regime the dynamics found in present work is indeed similar to the one of [38].

6. Conclusions

The present work reports experimental results on colloid-colloid and colloid-substrate adhesion for microbeads coated by a controlled amount f of temperature-responsive polymer chains, the latter grouped in patches. We used DLS and real time particle tracking within a temperature ramp from below to above the polymer collapse temperature, at which the particles become sticky. Our main result is that both aggregation and adsorption can be triggered by increasing temperature, that both are reversible and that stability ratio and soft adhesion stiffness can be finely tuned by f.

7. Acknowledgments

We thank Ken Sekimoto for stimulating and helpful discussions. This work was mainly supported by ANR DAPPlePur 13-BS08-0001-01. Authors benefited from access to zeta-potential measurement of "Institut Pierre-Gilles de Gennes (program “Investissements d’Avenir” ANR-10-EQPX-34) with the help of J. Fattacioli.

References

[1] J. Largo, P. Tartaglia, F. Sciortino, Effective nonadditive pair potential for lock-and-key interacting particles: The role of the limited valence, Physical Review E 76 (1) (2007) 011402. doi:10.1103/PhysRevE.76.011402.

[2] F. Sciortino, E. Zaccarelli, Reversible gels of patchy particles, Current Opinion in Solid State and Materials Science 15 (6) (2011) 246–253. doi:10.1016/j.cossms.2011.07.003.

[3] S. Gon, K.-N. Kumar, K. Nüsslein, M. M. Santore, How bacteria adhere to brushy peg surfaces: clinging to flaws and compressing the brush, Macromolecules 45 (20) (2012) 8373–8381. doi:10.1021/ma300981r.

[4] S. Gon, B. Fang, M. Santore, Interaction of cationic proteins and polypeptides with biocompatible cationically-anchored peg brushes, Macromolecules 44 (20) (2011) 8161–8168. doi:10.1021/ma201484h.

[5] J. C. Giddings, Field-flow fractionation: analysis of macromolecular, colloidal, and particulate materials, Science 260 (5113) (1993) 1456–1465. doi:10.1126/science.8502990.

[6] M. Martin, R. Beckett, Size selectivity in field-flow fractionation: Lift mode of retention with near-wall lift force, The Journal of Physical Chemistry A 116 (25) (2012) 6540–6551. doi:10.1021/jp212414e@proofing.

[7] R. Straube, M. Falcke, Reversible clustering under the influence of a periodically modulated binding rate, Physical Review E 76 (1) (2007) 010402. doi:10.1103/PhysRevE.76.010402.

[8] K. Bishop, B. Grzybowski, Localized chemical wave emission and mode switching in a patterned excitable medium, Physical review letters 97 (12) (2006) 128702. doi:10.1103/PhysRevLett.97.128702.

[9] C. Alvarez-Lorenzo, L. Bromberg, A. Concheiro, Light-sensitive intelligent drug delivery systems, Photochemistry and photobiology 85 (4) (2009) 848–860. doi:10.1111/j.1751-1097.2008.00530.x.

[10] S. Murdan, Electro-responsive drug delivery from hydrogels, Journal of controlled release 92 (1) (2003) 1–17. doi:10.1016/S0168-3659(03)00303-1.

[11] M. Zrinyi, Intelligent polymer gels controlled by magnetic fields, Colloid & Polymer Science 278 (2) (2000) 98–103. doi:10.1007/s003960050017.

[12] V. Tsyalkovsky, R. Burtovyy, V. Klep, R. Lupitskyy, M. Motornov, S. Minko, I. Luzinov, Fluorescent nanoparticles stabilized by poly (ethylene glycol) containing shell for ph-triggered tunable aggregation in aqueous environment, Langmuir 26 (13) (2010) 10684–10692. doi:10.1021/la101021t.

[13] M. Motornov, J. Zhou, M. Pita, I. Tokarev, V. Gopishetty, E. Katz, S. Minko, An integrated multifunctional nanosystem from command nanoparticles and enzymes, Small 5 (7) (2009) 817–820. doi:10.1002/smll.200801550.

[14] M. Motornov, R. Sheparovych, R. Lupitskyy, E. MacWilliams, S. Minko, Responsive colloidal systems: Reversible aggregation and fabrication of superhydrophobic surfaces, Journal of colloid and interface science 310 (2) (2007) 481–488. doi:10.1016/j.jcis.2007.01.052.

[15] M. Motornov, R. Sheparovych, R. Lupitskyy, E. MacWilliams, O. Hoy, I. Luzinov, S. Minko, Stimuli-responsive colloidal systems from mixed brush-coated nanoparticles, Advanced Functional Materials 17 (14) (2007) 2307–2314. doi:10.1002/adfm.200600934.

[16] F. Wang, L. Cheng, T. Chen, D. Zhu, Q. Wen, S. Wang, Facile preparation of polymeric dimers from amphiphilic patchy particles, Macromolecular rapid communications 33 (10) (2012) 933–937. doi:10.1002/marc.201100787.

[17] J. M. Horton, C. Bao, Z. Bai, T. P. Lodge, B. Zhao, Temperature-and ph-triggered reversible transfer of doubly responsive hairy particles between

water and a hydrophobic ionic liquid, Langmuir 27 (21) (2011) 13324–13334. doi:10.1021/la2031818.

[18] M. A. C. Stuart, W. T. Huck, J. Genzer, M. Müller, C. Ober, M. Stamm, G. B. Sukhorukov, I. Szleifer, V. V. Tsukruk, M. Urban, et al., Emerging applications of stimuli-responsive polymer materials, Nature materials 9 (2) (2010) 101–113. doi:10.1038/nmat2614.

[19] Y. Lu, Y. Mei, M. Drechsler, M. Ballauff, Thermosensitive core–shell particles as carriers for ag nanoparticles: modulating the catalytic activity by a phase transition in networks, Angewandte Chemie International Edition 45 (5) (2006) 813–816. doi:10.1002/anie.200502731.

[20] Y. Lu, S. Proch, M. Schrinner, M. Drechsler, R. Kempe, M. Ballauff, Thermosensitive core-shell microgel as a ìnanoreactorî for catalytic active metal nanoparticles, Journal of Materials Chemistry 19 (23) (2009) 3955–3961. doi:10.1039/B822673N.

[21] D. B. Lawrence, T. Cai, Z. Hu, M. Marquez, A. Dinsmore, Temperature-responsive semipermeable capsules composed of colloidal microgel spheres, Langmuir 23 (2) (2007) 395–398. doi:10.1021/la062676z.

[22] O. J. Cayre, N. Chagneux, S. Biggs, Stimulus responsive core-shell nanoparticles: synthesis and applications of polymer based aqueous systems, Soft Matter 7 (6) (2011) 2211–2234. doi:10.1039/C0SM01072C.

[23] M.-Q. Chen, T. Serizawa, M. Li, C. Wu, M. Akashi, et al., Thermosensitive behavior of poly (n-isopropylacrylamide) grafted polystyrene nanoparticles, Polymer journal 35 (12) (2003) 901–910. doi:10.1295/polymj.35.901.

[24] M.-Q. Zhu, L.-Q. Wang, G. J. Exarhos, A. D. Li, Thermosensitive gold nanoparticles, Journal of the American Chemical Society 126 (9) (2004) 2656–2657. doi:10.1021/ja038544z.

[25] Q. Zhao, N. Chen, D. Zhao, X. Lu, Thermoresponsive magnetic nanoparticles for seawater desalination, ACS applied materials & interfaces 5 (21) (2013) 11453–11461. doi:10.1021/am403719s.

[26] J. Malinge, F. Mousseau, D. Zanchi, G. Brun, C. Tribet, E. Marie, Tailored stimuli-responsive interaction between particles adjusted by straightforward adsorption of mixed layers of poly (lysine)-g-peg and poly (lysine)-g-pnipam on anionic beads, Journal of colloid and interface science 461 (2016) 50–55. doi:10.1016/j.jcis.2015.09.016.

[27] G. L. Kenausis, J. Vörös, D. L. Elbert, N. Huang, R. Hofer, L. Ruiz-Taylor, M. Textor, J. A. Hubbell, N. D. Spencer, Poly (l-lysine)-g-poly (ethylene glycol) layers on metal oxide surfaces: attachment mechanism and effects of polymer architecture on resistance to protein adsorption, The Journal of Physical Chemistry B 104 (14) (2000) 3298–3309. doi:10.1021/jp993359m.

[28] N.-P. Huang, R. Michel, J. Voros, M. Textor, R. Hofer, A. Rossi, D. L. Elbert, J. A. Hubbell, N. D. Spencer, Poly (l-lysine)-g-poly (ethylene glycol) layers on metal oxide surfaces: surface-analytical characterization and resistance to serum and fibrinogen adsorption, Langmuir 17 (2) (2001) 489–498. doi:10.1021/la000736+.

[29] S. Gon, M. Bendersky, J. L. Ross, M. M. Santore, Manipulating protein adsorption using a patchy protein-resistant brush, Langmuir 26 (14) (2010) 12147–12154. doi:10.1021/la1016752.

[30] C. Gosse, V. Croquette, Magnetic tweezers: micromanipulation and force measurement at the molecular level, Biophysical journal 82 (6) (2002) 3314–3329. doi:10.1016/S0006-3495(02)75672-5.

[31] M. Von Smoluchowski, Drei vortrage uber diffusion. brownsche bewegung und koagulation von kolloidteilchen, Z. Phys. 17 (1916) 557–585.

[32] J. S. T., W.-K. Zarah, B. S. J., H. S. L., del Barrio Jesus, S. O. A., The importance of excess poly(n-isopropylacrylamide) for the aggregation of poly(n-isopropylacrylamide)- coated gold nanoparticles, ACS Nano 10 (2016) 3158–3165. doi:10.1021/acsnano.5b04083.

[33] B. Sun, Y. Lin, P. Wu, H. W. Siesler, et al., A ftir and 2d-ir spectroscopic study on the microdynamics phase separation mechanism of the poly (n-isopropylacrylamide) aqueous solution, Macromolecules 41 (4) (2008) 1512–1520. doi:10.1021/ma702062h.

[34] S. Kalasin, M. M. Santore, Near-surface motion and dynamic adhesion during silica microparticle capture on a polymer (solvated peg) brush via hydrogen bonding, Macromolecules 49 (1) (2015) 334–343. doi:10.1021/acs.macromol.5b01977.

[35] C. Korn, U. Schwarz, Dynamic states of cells adhering in shear flow: from slipping to rolling, Physical review E 77 (4) (2008) 041904. doi:10.1103/PhysRevE.77.041904.

[36] M. Mani, A. Gopinath, L. Mahadevan, How things get stuck: Kinetics, elastohydrodynamics, and soft adhesion, Phys. Rev. Lett. 108 (2012) 226104. doi:10.1103/PhysRevLett.108.226104.
URL http://link.aps.org/doi/10.1103/PhysRevLett.108.226104

[37] K.-C. Chang, D. A. Hammer, The forward rate of binding of surface-tethered reactants: effect of relative motion between two surfaces, Biophysical Journal 76 (3) (1999) 1280–1292. doi:10.1016/S0006-3495(99)77291-7.

[38] D. Kumar, S. Bhattacharya, S. Ghosh, Weak adhesion at the mesoscale: particles at an interface, Soft Matter 9 (2013) 6618–6633. doi:10.1039/C3SM00097D.
URL http://dx.doi.org/10.1039/C3SM00097D

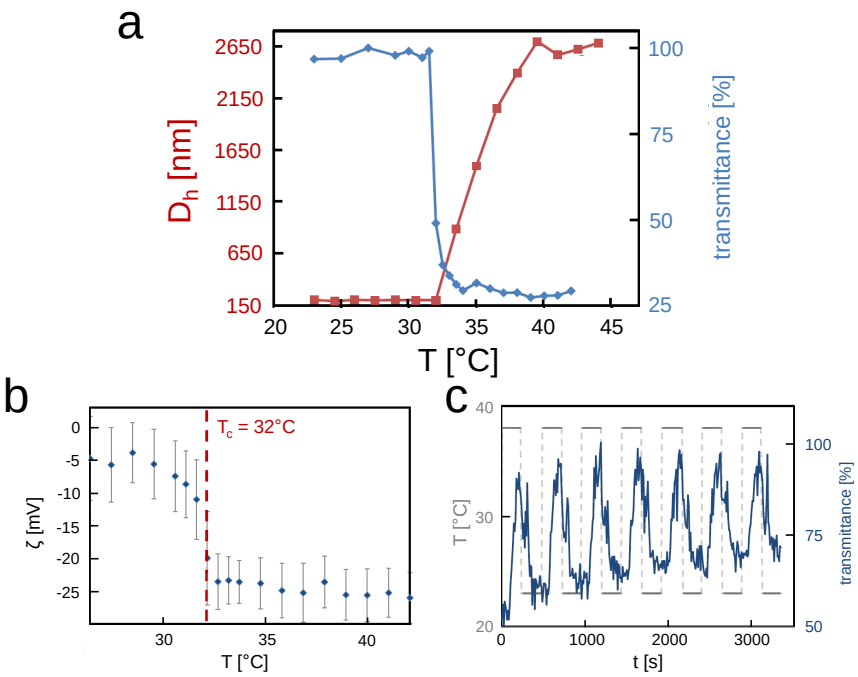

Figure 1: Temperature-triggered aggregation of coated 200 nm polystyrene beads. **a.** 100% PLL-g-PNIPAM coated particles show aggregation by the variation of the transmittance at 650 nm (blue line, right scale) and of the apparent hydrodynamic diameter measured by DLS at 90 ° angle (red line, left scale). Both the measurements are recorded during a +1°C temperature increment every 4 minutes. **b.** ζ-potential as a function of temperature for a bead saturated with PLL-g-PNIPAM (100% PLL-g-PNIPAM). **c.** Transmittance at 650 nm for a dispersion of 100% PLL-g-PNIPAM coated beads during heating/cooling cycles. Figure adapted from [26].

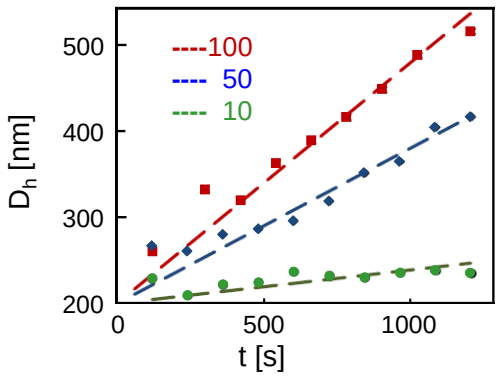

Figure 2: DLS measurements at 40°C for particles at PNIPAM fractions $f = 100\%$ (red squares), 50% (blue lozenges), 10% (green circles). Beads concentration $= 8.5 - 10.5 \mu g.L^{-1}$ in 5 mM phosphate buffer. Figure adapted from [26].

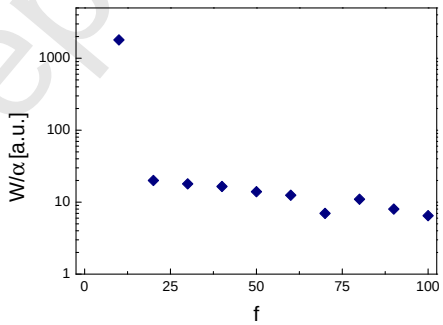

Figure 3: Stability ratio W, normalized by the numerical pre-factor α, as a function of PLL-g-PNIPAM surface fraction f. Figure adapted from [26].

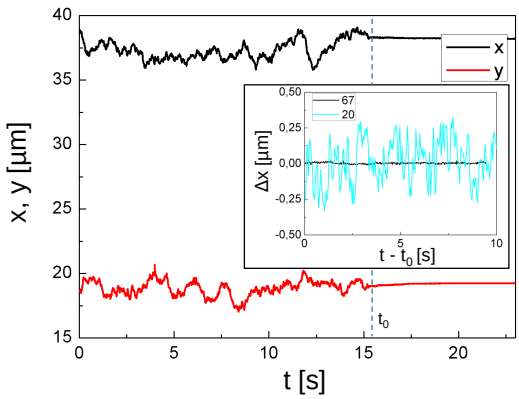

Figure 4: x-y tracking of a silica bead coated with a mixture PLL-g-PEG/PLL-g-PNIPAM (PNIPAM fraction: $f = 67\%$) during an increasing temperature ramp 10°C/min around the transition temperature. Transition between diffusive and adsorption regimes occurs at time t_0 (dashed line). Starting positions for x and y trajectories are arbitrary choices in the lab frame. Inset: detail of x profile in the adsorption regime. Two particle coatings ($f = 67\%, 20\%$) are shown for comparison.

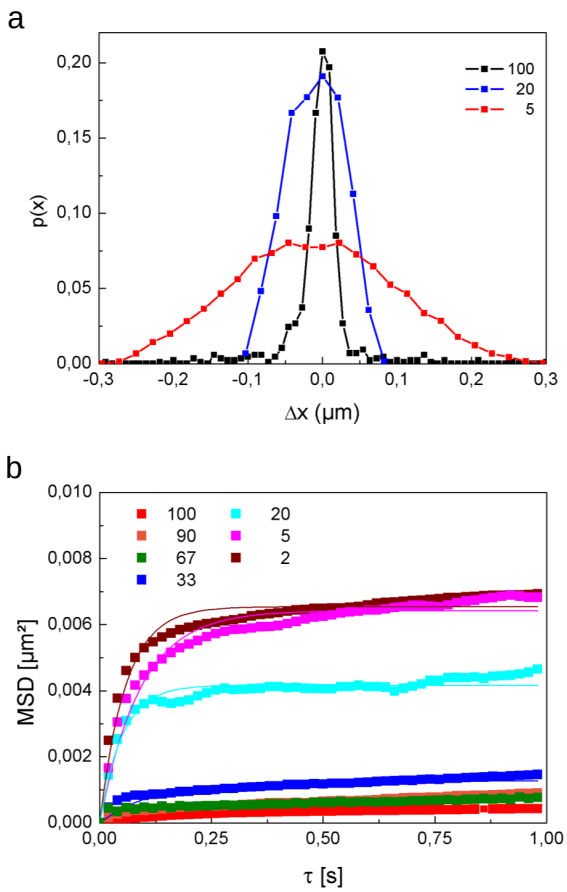

Figure 5: Confined fluctuations of softly attached particles **a.** Position distributions of particles adsorbed on the flat substrate: $f = 100\%$ (black), $f = 20\%$ (blue), $f = 5\%$ (red). Different widths suggest a f-dependent anchoring. **b.** MSD vs. time lag τ for adsorbed particles in the experimental range of f values. Thin lines are fits to formula in Eq.1, solution of Langevin equation in a harmonic potential well. The plateau value give us the "elasticity" constant α, whose best fitting values are shown in Fig.6.

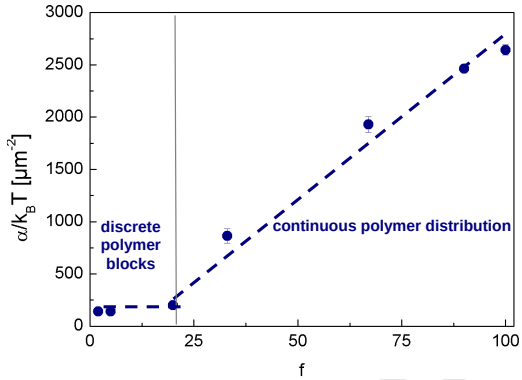

Figure 6: Coefficient α, as shown in Eq.1, vs. PNIPAM surface fraction f.

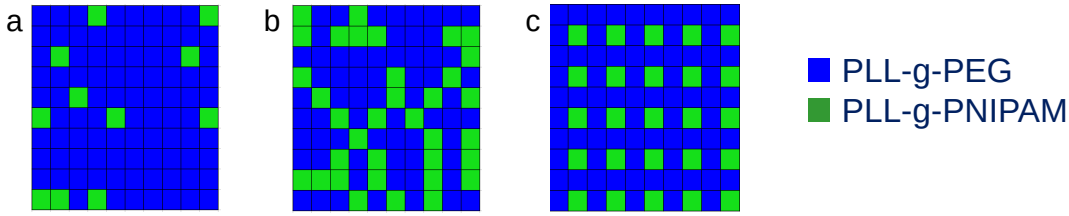

Figure 7: Schematic views of possible polymer arrangements on bead surface. Each square represents a PLL-g-PEG (blue) or PLL-g-PNIPAM (green) block adsorbed on silica. **a.** Random configuration at $f = 10\%$ showing isolated PLL-g-PNIPAM blocks. **b.** Random configuration at $f = 33\%$ with continuous PLL-g-PNIPAM zones. **c.** Configuration possible at $f = 25\%$ explaining the approximate threshold between the two regimes by percolation arguments.